TABLE II. Rates in sec^{-1} for the vibrational-rotational levels indicated and electrons ejected from the nth level. All results are in the Born approximation.

v_i	J_i	M_{Ji}	v_f	J_f	M_{Jf}	n	This theory (w V_{LR})	This theory (w/o V_{LR})
1	1	0	0	1	0	8	7.6×10^{11}	
1	1	0	0	1	1	8	3.5×10^{11}	
1	1	1	0	1	1	8	8.6×10^{10}	
	Averaged and summed						8.3×10^{11}	
	2	0		0	0	30		6.9×10^{9}
	2	1		0	0	30		3.0×10^{9}
	2	2		0	0	30		3.8×10^{10}
	Averaged							1.8×10^{10}
5	0	0	3	0	0	8		1.1×10^{11}
4	0	0	2	0	0	8		6.3×10^{10}
2	0	0	0	0	0	8		9.5×10^{9}

tron and nuclear velocities may be comparable but the contribution to the total magnitude of the rate in this region is not as large, although as stated above is quite important. Our conclusions may be summarized as follows. The rates of the Faisal calculation are fortuitously too low; these rates would be directly comparable to our rates *without* V_{LR} if the short-ranged part of the Hartree potential, V_{SR}, had been included. Note that these rates (w V_{LR}) show an agreement with the measured rates of Chupka and Berkowitz (CB) which are better, in general, than the rates calculated in the best representation of the potential (w V_{LR}). On the other hand, these "best" rates (w V_{LR}) show a consistently good agreement with the fully quantum-mechanical rates of the BN theory. This is a check on the accuracy of the semiclassical approximations made herein. Our rates are consistently larger than those of BN and in better agreement with experiment; disagreement with these rates may be due to errors inherent in the semiclassical approximation; however, it is also likely to arise from other sources such as choice of vibrator states and errors inherent in the perturbed-stationary-state theory, viz., the accuracy of the zeroth-order BO states and the accuracy of the Born approximation calculated in large nonadiabatic perturbations. Additional errors may arise from the choice of cutoff functions [Eqs. (12)].

[1]W. A. Chupka and J. Berkowitz, J. Chem. Phys. 51, 4244 (1969).
[2]J. N. Bardsley, Chem. Phys. Letters 1, 229 (1967).
[3]R. S. Berry, J. Chem. Phys. 45, 1228 (1966).
[4]B. Ritchie, Phys. Rev. A 3, 95 (1971).
[5]R. S. Berry and S. E. Nielsen, Phys. Rev. A 1, 395 (1970).
[6]F. H. M. Faisal, Phys. Rev. A 4, 1396 (1971).
[7]A. Temkin, Phys. Rev. 116, 358 (1959); A. Temkin and J. C. Lamkin, *ibid.* 121, 788 (1961).
[8]A. Russek, M. R. Patterson, and R. L. Becker, Phys. Rev. 167, 17 (1968).
[9]A. Rahman, Physica 19, 145 (1953).
[10]The quantum theory has been formulated for this case by U. Fano [Phys. Rev. A 2, 353 (1970)].

PHYSICAL REVIEW A VOLUME 6, NUMBER 5 NOVEMBER 1972

Interpretation of Photoabsorption in the Vicinity of the 3*d* Edges in La, Er, and Tm

Jack Sugar
National Bureau of Standards, Washington, D. C. 20234
(Received 10 July 1972)

Line spectra at the 3*d* photoabsorption edges of La, Er, and Tm are interpreted as transitions of the type $3d^{10}4f^N \rightarrow 3d^9 4f^{N+1}$. Calculated relative *gf* values for these transitions are compared with published absorption curves.

The penetration by the 4*f* wave function of the centrifugal potential barrier in the lanthanides ($57 \geq Z \geq 70$) has been invoked[1,2] to account for the rich photoabsorption resonance structure in the vicinity of, and far beyond, the 4*d* absorption edges. Extensive overlap of the 4*d* and 4*f* orbits results in a large exchange interaction and therefore a large splitting (10–20 eV) of the $4d^9 4f^{N+1}$ configu-

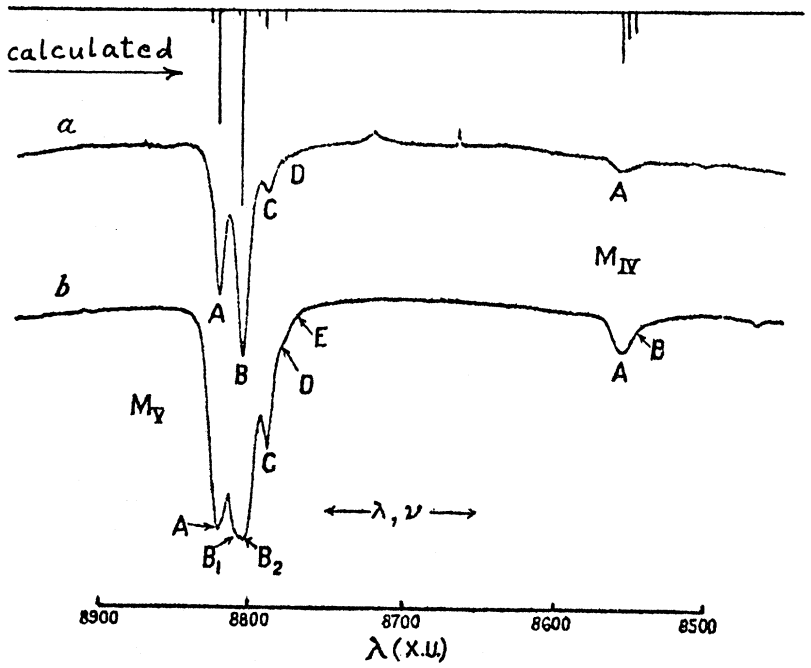

FIG. 1. Comparison between observed and calculated photoabsorption spectrum of erbium in the region of the M_{IV} and M_V edges. Experimental curves are from Ref. 4. The lines show calculated relative gf values.

ration formed by excitation of an electron from the $4d^{10}$ shell into the $4f^N$ shell. No edge structure is observed, since no higher members of the nf series ($n > 4$) penetrate the barrier and overlap the $4d$ wave function.[3] Thus, no buildup of a series limit (edge) takes place.

TABLE I. Calculated energies (in eV) and relative gf values of absorption lines in La, Er, and Tm metals near the $3d$ edges. In Er, lines less than 3% of maximum are omitted.

Transitions	E_{calc}	gf_{rel}	E_{obs}
La $3d^{10} \rightarrow 3d^9 4f$			
$^1S_0 \rightarrow {}^3P_1$	829.7	0.06	829.7
$^3D_1$	834.2	5.8	834.2
$^1P_1$	850.2	10.0	850.2
Er $3d^{10}4f^{11} \rightarrow 3d^9(4f^{12})$			
$^4I_{15/2} \rightarrow (^3H)^4K_{17/2}$	1405.1	0.6	
$(^3H)^4I_{15/2}$	1405.9	5.8	1405.9
$(^3H)^4K_{15/2}$	1407.4	0.3	
$(^3F)^4H_{13/2}$	1408.1	10.0	1408.1
$(^1I)^2I_{13/2}$	1409.2	0.3	
$(^1G)^2I_{13/2}$	1410.3	0.8	1410.3
$(^1I)^2K_{15/2}$	1411.9	0.4	
$(^3H)^4I_{13/2}$	1449.1	2.6	1449.1
$(^3H)^2I_{13/2}$	1449.6	1.3	
$(^3H)^2K_{15/2}$	1450.4	1.1	
Tm $3d^{10}4f^{12} \rightarrow 3d^9 4f^{13}$			
$^3H_6 \rightarrow {}^3H_6$	1463.6	3.4	1463.6
$^3G_5$	1465.5	10.0	1465.5
$^1H_5$	1467.7	1.7	
$^3H_5$	1509.8	2.2	

Photoabsorption in the vicinity of the $3d$ threshold also exhibits line structure,[4-7] but in this case the $3d^9$ spin-orbit interval is prominent; lines cluster about the expected positions of the M_{IV} and M_V edges. The penetration of the potential barrier by the $4f$ orbit is again responsible for these lines, but the overlap in this case is much less than with $4d$. Consequently, the line structure observed constitutes a small fraction of the total oscillator strength for $3d$ absorption. There is again no edge due to higher series members. It will be seen that all the observed features for the cases treated are accounted for by the $3d^9 4f^{N+1}$ configuration.

TABLE II. Values of the radial interaction integrals used in the diagonalization of the $3d^9 4f^{N+1}$ energy matrices. Standard errors are given for values fitted by least squares to observed data. All values are in eV.

	La $3d^9 4f$	Er $3d^9 4f^{12}$	Tm $3d^9 4f^{13}$
F^2	6.03	7.64	7.87
F^4	2.78	3.67	3.78
G^1	4.19 ± 0[a]	5.74 ± 0.04	5.98
G^3	2.44	3.43	3.50
G^5	1.68	2.59	2.41
ζ_d	6.45 ± 0	16.8 ± 0.06	17.85
ζ_f	0.080	0.327	0.330
E^1		0.896	
E^2		0.004	
E^3		0.084	

[a]The fit is exact for La since only two intervals between peaks are fitted with two free parameters.

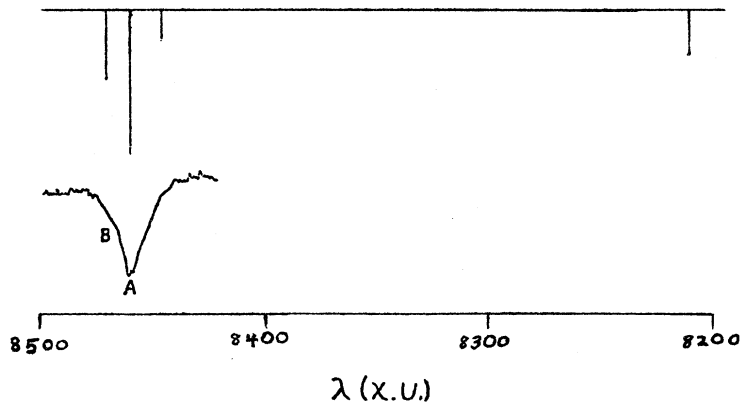

FIG. 2. Comparison between observed and calculated photoabsorption spectrum of thulium in the region of the M_{IV} and M_V edges. Experimental curve is from Ref. 6. Calculated relative gf values appear above curve.

I carried out a parametric calculation of the $3d$ absorption spectrum of Er that gives good agreement with the observations reported by Stewardson and Wilson.[4] A comparison between the experimental and theoretical results is shown in Fig. 1. Curves a and b (reproduced from Ref. 4) differ by the thickness of the absorbing metallic film, a being obtained with a 0.1-mg/cm^2 sample and b with a 0.3-mg/cm^2 sample. The strong peaks $A(M_V)$ and $B(M_V)$ of curve a have apparently become saturated in b, and the small peak at $D(M_V)$ is evident in b. There is no predicted line at $E(M_V)$ or double peak at B.

The computational methods and the physical model are the same as those used in Ref. 2 for the $4d$ excitations. In summary, the initial state is considered to be effectively a triply ionized free atom in the ground state. The energy matrices of the $3d^9 4f^{12}$ configuration of triply ionized Er were diagonalized with scaled Hartree–Fock (HF) values for the Slater integrals, a value for the $3d^9$ spin-orbit parameter estimated from the compilation of x-ray data by Bearden,[8] and values for the $4f^{12}$ interactions taken from Ref. 2. The resulting eigenvectors were used to transform calculated line strengths of the $3d^{10}4f^N \rightarrow 3d^9 4f^{N+1}$ transition array from LS to intermediate coupling so as to predict the experimental relative line strengths. The energy eigenvalues were then fitted to the observed peaks by adjusting the values of the radial coefficients $G^1(df)$ and ζ_d (the $3d^9$ spin-orbit parameter). After a fitted value of G^1 of about 65% of the HF value was obtained, all the other Slater integrals were reduced by the same amount. This is consistent with the fitting[2] of the $4d$ absorption data for Er, which required a reduction of the HF value of G^1 by 67%.

The Tm data are more sketchy. In 1952 Lee, Stewardson, and Wilson[5] reported the absorption curve shown in Fig. 2. It represents only the neighborhood of the M_V edge and shows evidence of two lines. In 1966 Williams[6] reported on the $M_{IV,V}$ spectra of Eu and remarked that Stewardson and Wilson had made new observations of Tm which revealed three lines at M_V and one at M_{IV}. The present calculation of Tm is given in Fig. 2 for comparison with the data of Ref. 5. It does indeed show four lines. No fitting was done, but the estimated interval[5] between A and B of ~2 eV is confirmed. For this calculation the HF–Slater parameters were reduced by 65%, in accordance with the Er results.

I also calculated the spectrum of La, fitting it to the experimental curve given by Fisher and Baun.[7] The relative intensities are in qualitative agreement with the data, but the fitted scaling of the HF integrals is 77% compared with 58% for G^1 in the $4d$ shell.

Reference 7 gives absorption curves for each of the lanthanide metals (except Pm). In some cases they are in disagreement with other published data and with the present theoretical model. Ytterbium has previously been found to have no absorption line in the pure metal and only one in the oxide.[9] This is consistent with the divalent nature of metallic Yb which leaves a closed $4f$ shell, and the trivalency of the oxide where the only possible absorption line is $3d^{10}4f^{13}\,{}^2F_{7/2} \rightarrow 3d^9 4f^{14}\,{}^2D_{5/2}$. In Ref. 7 there are four absorption peaks for Yb. The curve for Tm in Ref. 7 contains seven peaks where only four are allowed: $3d^{10}4f^{12}\,{}^3H_6 \rightarrow 3d^9 4f^{13}\,{}^3G_5$, ${}^1H_5$, ${}^3H_5$, ${}^3H_6$. On the other hand, the Er curve matches the data in Ref. 4, which is reproduced here in Fig. 1. There is a need for sorting out these discrepancies in the observations, or for further refinement of the model.

The calculated spectra for La, Er, and Tm are given in Table I. Table II contains the values of the radial integrals (the Slater F^k and G^k and the spin-orbit parameters ζ_d and ζ_f) used in diagonalizing the energy matrices.

[1]J. L. Dehmer, A. F. Starace, U. Fano, J. Sugar, and J. W. Cooper, Phys. Rev. Letters 26, 1521 (1971).
[2]J. Sugar, Phys. Rev. B 5, 1785 (1972).
[3]J. W. Cooper, Phys. Rev. Letters 13, 762 (1964).
[4]E. A. Stewardson and J. E. Wilson, Proc. Phys. Soc. (London) A69, 93 (1956).
[5]P. A. Lee, E. A. Stewardson, and J. E. Wilson, Proc. Phys. Soc. (London) A65, 668 (1952).
[6]K. C. Williams, Proc. Phys. Soc. (London) 87, 983 (1966).
[7]D. W. Fischer and W. L. Baun, Advan. X-Ray Anal. 11, 230 (1968).
[8]J. A. Bearden, Rev. Mod. Phys. 39, 78 (1967).
[9]F. H. Combley, E. A. Stewardson, and J. E. Wilson, J. Phys. B 1, 120 (1968).

PHYSICAL REVIEW A VOLUME 6, NUMBER 5 NOVEMBER 1972

Density-Matrix Study of Atomic Ground and Excited States. III. Geminal Energy Analysis of an Accurate Beryllium Ground-State Wave Function*

Pedro L. Olympia, Jr., Robert C. Morrison,† and Darwin W. Smith
Chemistry Department, University of Georgia, Athens, Georgia 30601
(Received 12 July 1971)

The total energy of an accurate beryllium ground-state wave function is decomposed into energies of its natural-spin geminals. These are further subdivided into kinetic, electron-nuclear attraction, and electron-electron interaction energy contributions. Similar subdivisions for a Hartree-Fock wave function are presented. It is pointed out that it is unreasonable to expect natural-spin geminals to be populated on the basis of their energies. The important energy implications of singlet-triplet degeneracies in a two-matrix are also discussed. The correlation energy is analyzed at the geminal level, and it is shown that the electron-nuclear attraction part of the correlation energy is negative and not negligible. For the beryllium ground state the Coulomb correlation energy is about four times greater than the Fermi correlation energy. It is pointed out that the Hartree-Fock wave function for beryllium contains too much Fermi correlation.

INTRODUCTION

A previous paper from this laboratory[1] presented an accurate beryllium wave function (referred to in the report as BeG1) accounting for nearly 96% of the correlation energy. The eigenvalues and eigenvectors of its first- and second-order density matrices were given, in part to illustrate the utility of density matrices as a global representation of a wave function, and to show how density matrices aid in the selection of orbital basis and configurations in a configuration-interaction (CI) scheme. The paper expressed the desirability of decomposing the total energy in terms of geminal energies. We have now completed this task and the present paper, as a first consideration, provides the answer to the question: How is the total energy partitioned among the natural-spin geminals (NSG's)? In attempting to answer this question one is led, partly as a matter of course, to a discussion of some aspects of the correlation problem, e.g., the Fermi and Coulomb correlation energies and their principal sources. In addition, we further subdivide each geminal energy into its various components: (i) the kinetic energy part T, (ii) the electron-nuclear attraction part V_1, and (iii) the electron interaction part V_{12}. By such a subdivision one hopes to gain a clearer understanding of the essential differences between geminals of a given wave function and corresponding geminals of the different wave functions. Since a similar subdivision can be made for Hartree-Fock (HF) geminals, one is afforded the opportunity to examine the components of the total correlation energy—in particular, the part due to the electron-nuclear attraction, whose sign apparently cannot be determined *a priori* from any quantum-mechanical argument.

Barnett and Platas[2] have previously reported the geminal energy decomposition of the Weiss Be wave function,[3] but their work is quite different from ours in content, emphasis, and purpose. In addition their work left some unanswered questions, on which we plan to elaborate and to which we attempt to give some answers.

COMPUTATIONS

In view of the fact that the Hamiltonian contains only one-particle operators ($T=\sum_i t_i$ and $V_1=\sum_i v_i$) and two-particle operators ($V_{12}=\sum_{ij(i<j)} v_{ij}$), the total energy can be obtained from the two-matrix. The natural expansion of the two-matrix is given by

$$\Gamma(12|1'2') = \sum_i \lambda_i g_i(12) g_i^*(1'2'), \tag{1}$$